Research Square

Preprints are preliminary reports that have not undergone peer review.
They should not be considered conclusive, used to inform clinical practice,
or referenced by the media as validated information.

Beyond landscape composition: configuration and landscape context shape sediment retention and delivery

Leting Lyu
Liaoning Normal University
Yan Niu
Liaoning Normal University
Mengjiao Hou
Liaoning Normal University
Defeng Zheng
defengzheng@lnnu.edu.cn
Liaoning Normal University
Feipeng Ren
Changjiang River Scientific Research Institute

Research Article

Keywords: landscape configuration, sediment retention rate, sediment delivery ratio, landscape context, Liao River Basin

Posted Date: November 16th, 2026

DOI: https://doi.org/10.21203/rs.3.rs-11550846/v1

License: This work is licensed under a Creative Commons Attribution 4.0 International License.
Read Full License

Additional Declarations: No competing interests reported.

Beyond landscape composition: configuration and landscape context shape sediment retention and delivery

Leting Lyu[1,2],Yan Niu[1],Mengjiao Hou[1],Defeng Zheng[1*],Feipeng Ren[3,4*]

[1.]College of Geosciences, Liaoning Normal University, Dalian 116029, China

[2.]Dalian Key Laboratory of Intelligent Management and Control of Land-Sea Agricultural Disasters, Liaoning Normal University, Dalian 116029, China

[3.]Changjiang River Scientific Research Institute, Changjiang Water Resources Commission, Wuhan 430010, China

[4.]Field Scientific Observation and Research Station of Aquatic Ecosystem in the Source Area of Changjiang River, Yushu, Qinghai 815000, China

Email: defengzheng@lnnu.edu.cn; feipengren2006@mail.bnu.edu.cn

telephone number：13214207618

Abstract

Context. Landscape composition and configuration represent distinct dimensions of spatial heterogeneity, yet their relative roles in regulating landscape–process relationships remain insufficiently understood. Sediment retention and delivery provide a useful process system for examining this question because both depend on the amount and spatial organization of land-cover elements.

Objectives. We examined the relative and complementary roles of landscape composition and configuration in explaining sediment retention and delivery, and further assessed whether these landscape–process relationships vary nonlinearly, among subbasins, and across contrasting landscape contexts.

Methods. We analyzed 30 years (1995–2024) of landscape-pattern and sediment-process data from 28 subbasins. Landscape composition and configuration were compared using panel-based explanatory models and grouped machine-learning validation. Nonlinear responses and subbasin-specific effects were further evaluated, and their variation was related to long-term land-cover backgrounds.

Results. Landscape configuration provided greater explanatory and predictive information than composition for both sediment retention and delivery. Metrics describing patch dominance, aggregation, edge structure, and fragmentation emerged as important configuration dimensions. Most key landscape–process relationships were dominated by overall associations, whereas significant nonlinearity was confined to a subset of relationships. The magnitude and, in some cases, direction of landscape effects also varied among subbasins. These subbasin-specific effects showed clearer dependence on long-term landscape context for sediment retention than for sediment delivery.

Conclusions. Sediment-related landscape–process relationships cannot be represented adequately by land-cover proportions alone. Integrating landscape composition, spatial configuration, and landscape context provides a more complete framework for understanding how spatial heterogeneity is associated with sediment retention and delivery across heterogeneous watersheds.

Keywords landscape configuration · sediment retention rate · sediment delivery ratio · landscape context · Liao River Basin

1. Introduction

The relationship between spatial landscape patterns and ecological processes has long been a central theme in landscape ecology. Spatial heterogeneity determines not only the amount and types of ecological elements within a landscape, but also the movement of materials, energy, and organisms among them (Turner, 1989; Levin, 1992; Pickett and Cadenasso, 1995). Landscape pattern is commonly characterized by two related but ecologically distinct dimensions: landscape composition, which describes the amount and proportion of different land-cover types, and landscape configuration, which describes their patch size, shape, aggregation, edge structure, and spatial arrangement. This distinction is particularly relevant to sediment processes in watersheds. Once sediment is generated in source areas, it may undergo hillslope transport, local deposition, remobilization, and eventual delivery to stream networks and watershed outlets. Therefore, sediment retention and delivery depend not only on the amount of potential source and sink areas, but also on how these landscape elements are spatially organized. Sediment redistribution thus provides a representative pattern–process system for examining how landscape structure is associated with material transfer across heterogeneous landscapes.

Previous studies have shown that land-cover composition is closely associated with soil erosion and sediment export, yet describing landscapes solely by the proportions of forest, cropland, or artificial surfaces may overlook important spatial information. Similar changes in land-cover area can produce different erosion and sediment responses when they occur under contrasting slope conditions, soil properties, or positions relative to stream networks (Bakker et al., 2008). Studies based on source–sink concepts have further demonstrated that landscape composition, spatial configuration, and transport pathways from sediment sources to streams jointly contribute to variation in sediment delivery ratio and sediment yield (Yang et al., 2012). Configuration metrics such as LPI, AI, CONTAG, and COHESION have also been associated with variation in soil erosion and sediment export (Shi et al., 2013). More recent studies have emphasized that landscape composition and configuration represent distinct but complementary dimensions of spatial heterogeneity and should therefore be considered jointly when examining erosion, sediment yield, and other watershed material fluxes (Weller et al., 2023; Zhang et al., 2024; Valladares-Castellanos et al., 2026). However, their relative and complementary roles in long-term sediment retention and delivery remain insufficiently resolved, particularly with respect to which dimensions of spatial configuration contain information not represented by land-cover proportions alone.

This question is further complicated by the strong spatial heterogeneity inherent in sediment-transfer processes. Early work recognized that only a fraction of eroded sediment ultimately reaches watershed outlets because sediment may be stored, remobilized, or redistributed within the watershed (Walling, 1983). The concept of sediment connectivity subsequently provided a framework for describing the degree of linkage among sediment sources, hillslopes, channels, and outlets, emphasizing that sediment transfer is associated both with source characteristics and with landscape resistance and spatial organization along transport pathways (Borselli et al., 2008; Fryirs, 2013; Cavalli et al., 2013; Bracken et al., 2015). Land-use change may also reorganize these connectivity relationships and thereby be associated with changes in sediment delivery (Liu et al., 2021). These findings suggest that a given landscape pattern may not correspond to a uniform process response across contrasting spatial settings. Landscape–process relationships may vary nonlinearly along landscape-structure gradients and may also differ in magnitude or even direction among subbasins with

contrasting forest, grassland, or impervious-surface backgrounds. Nevertheless, most previous studies have focused primarily on average landscape responses, whereas the combined roles of nonlinearity, subbasin-level spatial heterogeneity, and long-term landscape-context dependence have received comparatively less attention.

Accordingly, we treated subbasins as functional landscape units linking spatial heterogeneity with hillslope-to-stream sediment redistribution and used long-term landscape-pattern and sediment-process data to examine the relationships of landscape composition and configuration with the sediment retention service ratio (SRSR) and sediment delivery ratio (SDR). Specifically, we addressed three questions: (1) What are the relative and complementary roles of landscape composition and configuration in explaining sediment retention and delivery? (2) Do key landscape–process relationships exhibit nonlinear responses and significant variation among subbasins? and (3) Are subbasin-specific landscape effects associated with long-term landscape context? By integrating composition–configuration comparisons, nonlinear responses, spatial heterogeneity, and landscape-context dependence within a unified analytical framework, this study aims to advance understanding of the relationships between spatial landscape patterns and sediment retention and delivery across heterogeneous watersheds.

2. Materials and methods

We used subbasins as the basic analytical units. The InVEST Sediment Delivery Ratio (SDR) model was first applied to estimate soil erosion, sediment export, and sediment retention during 1995–2024, from which the sediment retention service ratio (SRSR) and sediment delivery ratio (SDR) were derived at the subbasin scale. Landscape pattern was then quantified from two complementary dimensions, landscape composition and landscape configuration. We subsequently compared their relative and complementary roles, identified key landscape metrics, evaluated nonlinear responses, and examined subbasin-level spatial heterogeneity and associations with long-term landscape context.

2.1 Study area and data sources

The Liao River Basin is located in northeastern China (116°50′–125°35′ E, 40°30′–45°10′ N) and covers approximately 2.15×10^5 km² (Fig. 1). Topography is generally higher on the eastern and western margins and lower in the central basin, with mountains and hills dominating the east and west and the Liao River Plain occupying the central region. The basin has a temperate monsoon climate, with annual precipitation of approximately 450–850 mm, decreasing from southeast to northwest; about 70% of annual precipitation occurs from June to September. The spatial interspersion of forest, cropland, grassland, and impervious surfaces creates pronounced landscape heterogeneity.

We used digital elevation model (DEM), precipitation, soil, and annual land-cover data (Table 1). The DEM and land-cover data had a spatial resolution of 30 m; annual land cover for 1995–2024 was obtained from the China Land Cover Dataset (CLCD). Precipitation data had an original resolution of 1 km, and soil data were obtained from the Harmonized World Soil Database (HWSD). All spatial datasets were projected to WGS 1984 UTM Zone 51N and resampled to 30 m. Subbasins were delineated using the DEM and observed river network, and annual InVEST outputs were matched with landscape metrics by subbasin, yielding a balanced panel of 28 valid subbasins × 30 years (1995–2024).

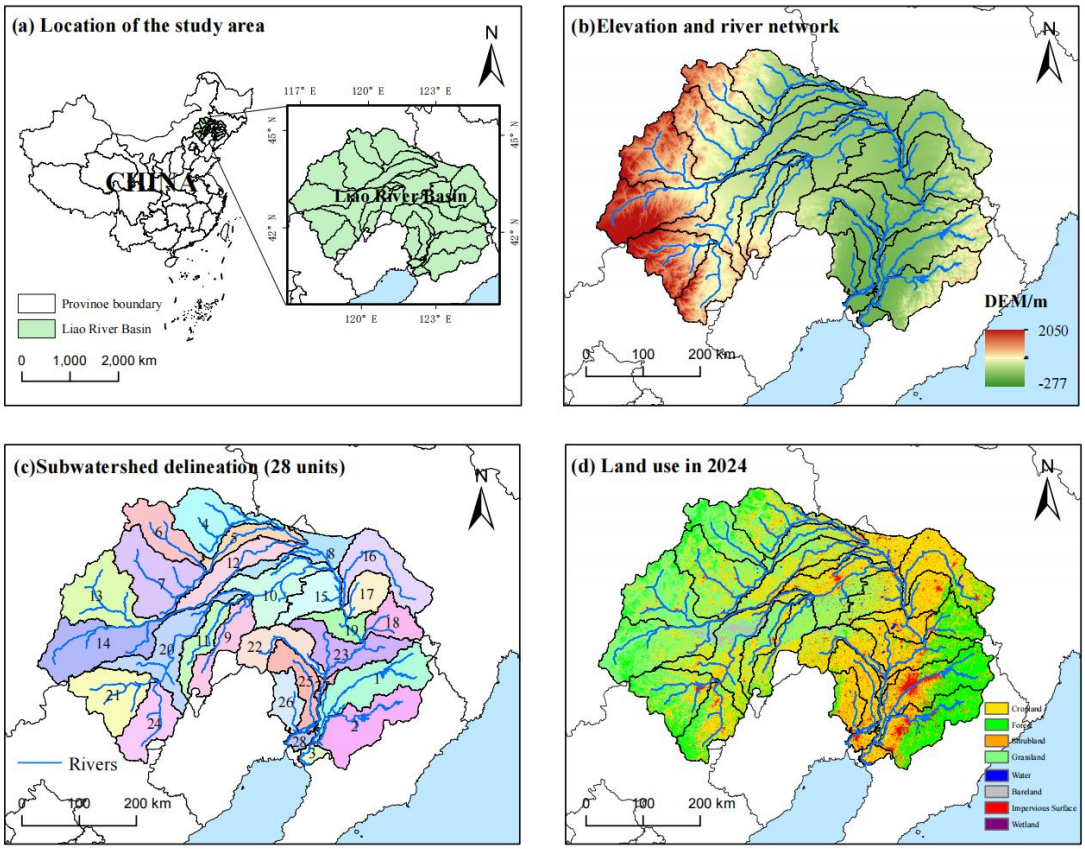


Fig. 1 Location, topography, subbasin delineation, and land-use characteristics of the study area (a) Location of the study area in northeastern China; (b) elevation and river network of the study area; (c) delineation and numbering of subbasins; and (d) land-use distribution in 2024

Table 1 Basic datasets used in this study and their applications

Dataset	Period	Original resolution/scale	Source	Application
DEM	—	30 m	Geospatial Data Cloud	Subbasin delineation and topographic factors
Precipitation	1995–2024	1 km	Resource and Environmental Science Data Center, CAS	Rainfall erosivity (R)
Soil	—	1:1,000,000	HWSD	Soil erodibility (K)
Land cover	1995–2024	30 m	CLCD, Wuhan University	C and P factors; landscape metrics

2.2 Sediment modelling and response metrics

2.2.1InVEST-SDR modelling

The InVEST Sediment Delivery Ratio (SDR) module was used to estimate hillslope soil erosion, sediment delivery, and sediment retention services during the study period (Hamel et al., 2015). Pixel-scale annual soil loss was first estimated using the Universal Soil Loss Equation framework:

$$USLE=R\times K\times LS\times C\times P \quad (1)$$

where R, K, LS, C, and P represent rainfall erosivity, soil erodibility, slope length and steepness, cover-management, and support-practice factors, respectively. The model then combines DEM-derived flow pathways, slope, land-cover resistance, and downslope pathways to the stream network to quantify sediment connectivity and convert it to a pixel-scale SDR, from which sediment export is

estimated. InVEST also estimates avoided sediment export, representing the sediment prevented from reaching the stream network through reduced local erosion and interception of upslope sediment under existing vegetation and land-management conditions. Model structure and parameterization followed Hamel et al. (2015).

2.2.2 Construction of SRSR and SDR

To distinguish landscape associations with sediment retention and sediment delivery, we constructed the sediment retention service ratio (SRSR) and sediment delivery ratio (SDR) at the subbasin scale. SRSR was defined as:

$$SRSR_{j,t}=\frac{avoid_exp_{j,t}}{avoid_exp_{j,t}+sed_export_{j,t}}\times 100\% \quad (2)$$

where $avoid_exp_{j,t}$ is the amount of sediment prevented from reaching the stream network under existing land-cover and management conditions in subbasin j and year t, and $sed_export_{j,t}$ is the amount of sediment delivered to the stream network. SRSR represents the proportion retained by existing land cover and landscape resistance relative to the sum of avoided and exported sediment, and therefore characterizes sediment retention within the landscape. SDR was defined as:

$$SDR_{j,t}^{sub}=\frac{sed_\mathrm{export}_{j,t}}{usle_\mathrm{tot}_{j,t}}\times 100\% \quad (3)$$

where $usle_tot_{j,t}$ is the actual soil erosion estimated under existing land-cover and management conditions in subbasin j and year t. SDR represents the proportion of eroded sediment ultimately delivered to the stream network and more directly reflects hillslope-to-stream sediment delivery efficiency. Because SRSR and SDR use different denominators, they are not strict mathematical complements.

2.3 Landscape composition and configuration metrics

Landscape patterns were characterized from the complementary dimensions of landscape composition and landscape configuration using the FRAGSTATS metric system (McGarigal and Marks, 1995; Uuemaa et al., 2009). Landscape composition was represented by the percentage of landscape (PLAND) occupied by forest, cropland, grassland, and impervious surfaces, whereas landscape configuration described patch dominance, fragmentation, edge structure, aggregation, and connectivity. At the class level, PLAND, PD, LPI, ED, AI, COHESION, and DIVISION were calculated; at the landscape level, L_PD, L_LPI, L_ED, L_AI, L_COHESION, L_DIVISION, L_CONTAG, and L_SHDI were calculated, yielding 36 landscape metrics in total (Table 2). The four PLAND metrics constituted the landscape-composition block, whereas the 24 non-PLAND class-level metrics and eight landscape-level metrics constituted the landscape-configuration block. For process interpretation, LPI represented dominant-patch importance; PD and DIVISION represented fragmentation and subdivision; ED represented edge structure; AI represented within-class aggregation; COHESION represented physical connectivity; and CONTAG represented landscape-level aggregation and interspersion.

Table 2 Landscape metrics used in this study and their ecological interpretations

Metric	Abbreviation	Level	Unit/range	Ecological interpretation
Percentage of landscape	PLAND	Class level	%	Percentage of a given land-use type in the total subbasin area; represents landscape composition.
Patch density	PD	Class and landscape levels	patches·100 ha^{-1}	Number of patches per unit area; higher values generally indicate greater landscape fragmentation.
Largest patch index	LPI	Class and landscape	%	Percentage of the total landscape area occupied by the largest patch; reflects

		levels		the dominance of the largest patch.
Edge density	ED	Class and landscape levels	$m \cdot ha^{-1}$	Patch-edge length per unit area; reflects edge development and spatial subdivision.
Aggregation index	AI	Class and landscape levels	0–100	Degree of aggregation among like pixels; higher values indicate stronger spatial aggregation of patches.
Patch cohesion index	COHESION	Class and landscape levels	0–100	Describes the physical connectedness and overall connectivity of patches; higher values indicate stronger connectivity.
Landscape division index	DIVISION	Class and landscape levels	0–1	Degree to which the landscape is divided into separate patches; higher values indicate greater subdivision.
Contagion index	CONTAG	Landscape level	%	Describes the aggregation and spatial extension of different patch types; higher values indicate a more aggregated overall landscape.
Shannon's diversity index	SHDI	Landscape level	≥0	Integrates landscape-type richness and evenness; higher values indicate greater landscape heterogeneity.

Note: Class-level metrics were calculated separately for forest, cropland, grassland, and impervious surfaces. The final analysis included 36 metrics: 4 land-cover classes × 7 class-level metrics (PLAND, PD, LPI, ED, AI, COHESION, and DIVISION) plus 8 landscape-level metrics (L_PD, L_LPI, L_ED, L_AI, L_COHESION, L_DIVISION, L_CONTAG, and L_SHDI). Metric definitions followed the FRAGSTATS framework (McGarigal and Marks, 1995; Uuemaa et al., 2009)

2.4 Temporal dynamics and relative importance of landscape pattern

2.4.1 Long-term changes in landscape and sediment processes

Long-term monotonic trends in landscape patterns, SRSR, and SDR during 1995–2024 were evaluated using the Mann–Kendall test, and rates of change were estimated using Sen's slope. Watershed-scale annual landscape metrics were summarized using subbasin-area-weighted means. For SRSR and SDR, both the subbasin median and an integrated watershed-scale ratio were calculated; the latter was derived from aggregated sediment fluxes. At the subbasin scale, long-term means and trends were calculated for each subbasin to characterize spatial heterogeneity in landscape patterns and sediment processes. All significance tests were two-sided, with $p < 0.05$ considered statistically significant.

2.4.2 Comparing landscape composition and configuration and identifying key metrics

To compare the relative and complementary roles of landscape composition and configuration in explaining sediment retention and delivery, we used two complementary analytical pathways: two-way fixed-effects (TWFE) models and grouped machine-learning cross-validation(Zheng et al., 2026). Landscape composition was represented by the four PLAND metrics for forest, cropland, grassland, and impervious surfaces, whereas landscape configuration comprised 24 non-PLAND class-level metrics and eight landscape-level metrics.

Using the balanced panel of 28 subbasins from 1995 to 2024, we fitted composition-only, configuration-only, and combined composition–configuration models while controlling for subbasin and year fixed effects. Within-R^2 and adjusted within-R^2 were used to compare the explanatory information associated with each landscape block for long-term within-subbasin variation. Incremental explanatory contributions were then calculated to quantify the additional information provided by one landscape block after accounting for the other. Leave-one-subbasin-out sensitivity analysis was used to assess whether the comparison was driven by any single spatial unit.

$$\Delta R^2 config|comp = R^2 combined - R^2 composition \quad (4)$$

$$\Delta R^2 comp|config = R^2 combined - R^2 configuration \quad (5)$$

Using the same composition, configuration, and combined predictor sets, we additionally fitted Random Forest, XGBoost, and LightGBM models. Five-fold cross-validation was grouped by subbasin so that observations from the same subbasin could not occur in both training and test sets. Out-of-fold R^2 was the primary performance metric, with RMSE and MAE used as supplementary measures. SHAP values from the combined models were used to quantify the relative predictive contribution of individual landscape metrics; importance values were normalized within each algorithm and then averaged across the three algorithms. The union of the top SHAP-ranked metrics for SRSR and SDR yielded key landscape metrics for subsequent analyses. Relative composition–configuration performance was evaluated primarily from TWFE and grouped cross-validation, whereas SHAP was used to identify specific influential metrics and the spatial dimensions they represented.

2.5 Nonlinear and spatially heterogeneous landscape effects

2.5.1Nonlinear pattern–process relationships

For the key landscape metrics identified above, two-way fixed-effects restricted cubic spline (TWFE-RCS) models were used to characterize their relationships with SRSR and SDR (Durrleman and Simon, 1989; Desquilbet and Mariotti, 2010). The model was specified as:

$$Yit = \alpha i + \gamma t + f(Xit) + \beta Zit + \varepsilon it \quad (6)$$

whereas composition metrics were adjusted for the remaining land-cover composition variables. Knots were placed at the 5th, 35th, 65th, and 95th percentiles of each focal metric, and standard errors were clustered at the subbasin level. Overall association and nonlinear spline components were tested for all metric–response relationships, with Benjamini–Hochberg FDR correction applied separately to the two sets of tests. Fitted curves were used to characterize response direction and shape, and a relationship was classified as nonlinear only when the nonlinear component remained significant after FDR correction. The fitted contrast between the 5th and 95th percentiles (Q5–Q95 Δ) was also reported as a descriptive effect size but was not used to determine nonlinear significance.

2.5.2 Subbasin-specific effects

Random-slope mixed-effects models were used to evaluate among-subbasin variation in the effects of key landscape metrics. Each metric was decomposed using the Mundlak approach into within-subbasin annual variation (within) and between-subbasin long-term differences (between), and both components were standardized to distinguish temporal variation from spatial background differences (Mundlak, 1978; van de Pol and Wright, 2009). For each focal metric, the within component was represented by a natural cubic spline (df = 5), while its between component, the within/between components of the other selected key metrics, and year effects were included as covariates. Models included a subbasin random intercept and a random slope for the focal within component. Random-slope heterogeneity was evaluated using likelihood-ratio tests with Benjamini–Hochberg FDR correction. Subbasin-specific effects were then quantified as the predicted change in SRSR or SDR when the focal metric increased from its subbasin-specific 10th to 90th percentile and were used in subsequent analyses of spatial heterogeneity and landscape-context dependence.

2.6 Landscape-context dependence

Long-term landscape context was represented by the 1995–2024 mean PLAND of forest, cropland, grassland, and impervious surfaces in each subbasin, and its associations with subbasin-specific effects of key landscape metrics were evaluated. For class-level metrics, effects were related to the long-term PLAND of the corresponding land-cover class; for landscape-level metrics, effects were evaluated

against the four PLAND backgrounds separately. Long-term land-use background may covary with pattern–process relationships through differences in source–sink configuration and sediment connectivity (Liu et al., 2021; Valladares-Castellanos et al., 2026). Spearman rank correlation was used as the primary test, with Pearson and Kendall correlations used as robustness checks. Benjamini–Hochberg FDR correction was applied separately to SRSR and SDR. LOWESS smoothing was used only to visualize overall trends and did not contribute to significance testing.

3. Results

3.1 Long-term landscape reorganization across the watershed

3.1.1 Changes in landscape composition

From 1995 to 2024, watershed land-cover composition was characterized by forest recovery, impervious-surface expansion, and cropland reduction (Fig. 2a). Forest_PLAND increased significantly from 13.13% to 14.59%, while Impervious_PLAND also increased significantly from 3.43% to 5.78%, representing the largest relative increase. Over the same period, Cropland_PLAND decreased from 49.04% to 47.31%, whereas Grassland_PLAND changed little (30.31% to 30.39%). Overall, landscape composition shifted from a relatively stable cropland-dominated pattern toward a land-use reorganization characterized by concurrent forest recovery, cropland adjustment, and impervious-surface expansion. These compositional changes showed pronounced spatial variation (Fig. 3a, b). Forest recovery was concentrated mainly in several western and southern subbasins, whereas impervious-surface expansion showed greater spatial consistency. In contrast, the direction and magnitude of cropland and grassland changes varied more strongly among subbasins, indicating marked regional differentiation in long-term land-use change.

3.1.2 Changes in landscape configuration

In addition to changes in landscape composition, landscape configuration also underwent substantial reorganization across the watershed (Fig. 2b). Landscape-level patch density (L_PD) decreased significantly from 11.82 to 8.53, and edge density (L_ED) decreased from 66.08 to 55.13 m ha^{-1}, indicating overall reductions in patch number and landscape edge. Meanwhile, the aggregation index (L_AI) increased significantly from 90.05 to 91.69, whereas the largest patch index (L_LPI) declined from 51.74 to 44.13 and the landscape division index (L_DIVISION) increased from 0.662 to 0.727. Together, these changes indicate that the landscape did not simply become more aggregated or more fragmented; rather, it showed a compound reorganization characterized by fewer patches and edges, stronger local aggregation, lower dominance of the largest patch, and greater landscape subdivision.

Class-level configuration changes further illustrated the sources of this spatial reorganization (Fig. 2c). Alongside the increase in forest area, Forest_LPI and Forest_AI also increased significantly, indicating expansion of dominant forest patches and stronger spatial aggregation. Impervious-surface expansion showed a more consistent composition–configuration shift: both Impervious_LPI and Impervious_AI increased, indicating the emergence of larger and more aggregated impervious patches. Spatially, decreases in L_PD and increases in L_AI were relatively consistent across subbasins, whereas the magnitudes of change in Forest_PLAND, Impervious_PLAND, and their key configuration metrics varied markedly among subbasins (Fig. 3). Overall, the Liao River Basin experienced long-term landscape reorganization involving concurrent changes in landscape composition and configuration from 1995 to 2024. Changes in land-cover proportions were accompanied by shifts in patch dominance, aggregation, and fragmentation.

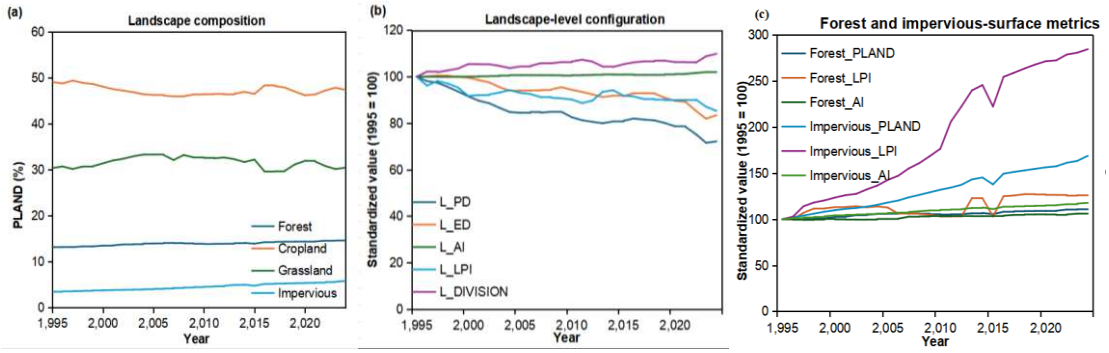


Fig. 2 Long-term changes in landscape composition and spatial configuration across the watershed during 1995–2024

(a) Annual proportions of forest, cropland, grassland, and impervious surfaces; (b) standardized changes in landscape-level patch density (L_PD), edge density (L_ED), aggregation index (L_AI), largest patch index (L_LPI), and landscape division index (L_DIVISION); and (c) standardized changes in key composition and configuration metrics of forest and impervious surfaces. Metrics in panels (b) and (c) were standardized relative to their 1995 values, with 1995 set to 100

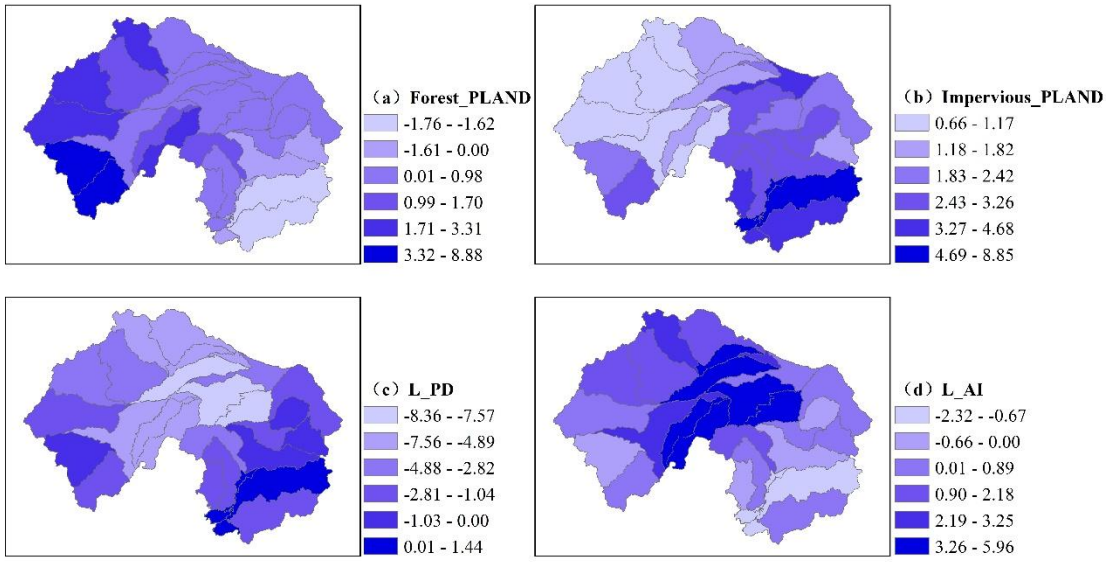


Fig. 3 Subbasin-level variation in changes in key landscape composition and spatial configuration metrics during 1995–2024

(a) Change in forest proportion (Forest_PLAND); (b) change in impervious-surface proportion (Impervious_PLAND); (c) change in landscape-level patch density (L_PD); and (d) change in landscape-level aggregation index (L_AI). Changes were calculated as the 2024 value minus the corresponding 1995 value. Forest_PLAND and Impervious_PLAND are expressed in percentage points, L_PD in patches per 100 ha, and L_AI in index points

3.2 Spatiotemporal dynamics of sediment retention and delivery

3.2.1 Long-term changes in sediment retention and delivery efficiency

From 1995 to 2024, the sediment retention service ratio (SRSR) showed a significant upward trend (Fig. 4a). The median subbasin SRSR increased from 97.473% to 97.784% (Kendall's $\tau = 0.867$, $p < 0.001$), while the integrated watershed-scale SRSR increased from 97.643% to 97.760% ($\tau = 0.407$, $p = 0.001$). In contrast, the sediment delivery ratio (SDR) declined significantly (Fig. 4b): the median subbasin SDR decreased from 2.717% to 2.424% ($\tau = -0.913$, $p < 0.001$), and the integrated watershed-scale SDR decreased from 3.386% to 3.059% ($\tau = -0.623$, $p < 0.001$). Overall, sediment retention increased over the study period, whereas the efficiency of hillslope sediment delivery to the stream network declined. Actual soil erosion, sediment export, and avoided sediment export showed

pronounced interannual variability but no significant long-term monotonic trends (Fig. 4c; p = 0.188, 0.697, and 0.227, respectively). Thus, long-term changes in sediment processes were expressed mainly through shifts in retention and delivery efficiency rather than persistent reductions in absolute soil erosion or sediment fluxes.

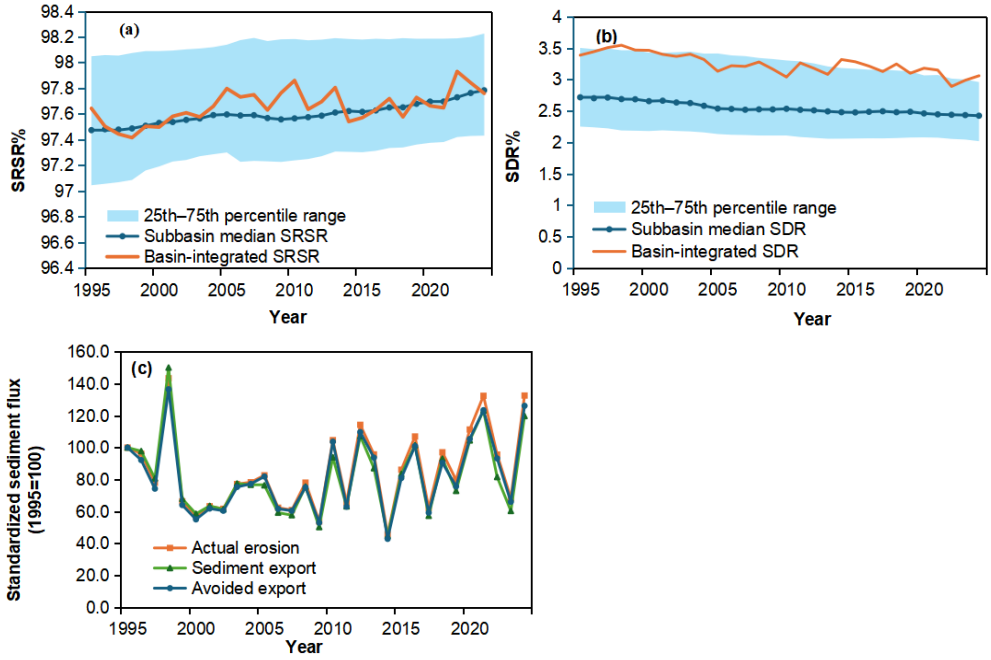


Fig. 4 Long-term changes in sediment retention service ratio, sediment delivery ratio, and absolute sediment fluxes during 1995–2024
(a) Median and interquartile range of subbasin SRSR together with the integrated watershed-scale SRSR; (b) median and interquartile range of subbasin SDR together with the integrated watershed-scale SDR; and (c) standardized interannual changes in actual soil erosion, sediment export, and avoided sediment export (1995 = 100). Integrated watershed-scale ratios were calculated from aggregated subbasin sediment fluxes rather than by averaging subbasin ratios

3.2.2 Spatial heterogeneity and sub-watershed trends

Both SRSR and SDR exhibited pronounced spatial variation among subbasins (Fig. 5a, b). Long-term mean SRSR ranged from 96.36% to 98.98%, with higher values mainly in eastern, southeastern, and parts of the south-central basin. Long-term mean SDR ranged from 1.74% to 4.27% and showed a broadly contrasting spatial pattern, with higher values concentrated mainly in western, northwestern, and northern subbasins. In general, subbasins with higher sediment retention tended to have lower sediment delivery efficiency; however, because SRSR and SDR are calculated using different reference quantities, they are not strict mathematical complements. Long-term trends also varied spatially (Fig. 5c, d). SRSR increased in most subbasins, whereas SDR generally decreased; significant increases in SRSR occurred in 22 subbasins and significant decreases in SDR in 26 subbasins. Stronger increases in SRSR and declines in SDR were concentrated mainly in western, northwestern, and some southern subbasins, whereas changes were weaker in parts of the eastern and southeastern high-retention areas. Overall, the basin showed a broadly consistent pattern of increasing sediment retention and decreasing sediment delivery from 1995 to 2024, but the magnitude of change varied markedly among subbasins.

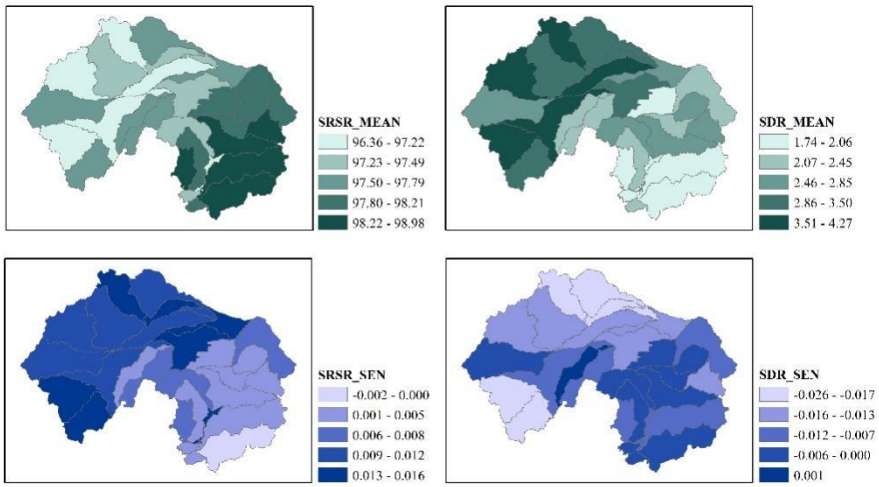


Fig. 5 Spatial patterns and long-term trends in sediment retention service ratio and sediment delivery ratio across sub-watersheds during 1995–2024
(a) Long-term mean sediment retention service ratio (SRSR); (b) long-term mean sediment delivery ratio (SDR); (c) Sen's slope of SRSR; and (d) Sen's slope of SDR. Sen's slope are expressed in percentage points yr^{-1}

3.3 Landscape pattern effects on sediment retention and delivery

3.3.1 Relative contributions of composition and configuration

Two-way fixed-effects models showed that landscape configuration accounted for more long-term within-subbasin variation in both SRSR and SDR than landscape composition (Fig. 6a). For SRSR, the within-R^2 values of the composition, configuration, and combined models were 0.243, 0.496, and 0.588, respectively; for SDR, the corresponding values were 0.133, 0.268, and 0.322. After accounting for differences in model dimensionality, adjusted within-R^2 remained higher for configuration than for composition (SRSR: 0.476 vs. 0.240; SDR: 0.239 vs. 0.129).

Incremental explanatory analysis showed that adding configuration to composition increased within-R^2 by 0.345 for SRSR and 0.189 for SDR, whereas adding composition to configuration increased within-R^2 by only 0.092 and 0.054, respectively. Relative to the explanatory information in the combined models, the independent contribution of configuration accounted for 58.6% of the explained information for SRSR and 58.7% for SDR, compared with 15.6% and 16.7% for composition; approximately one quarter of the information was shared. In leave-one-subbasin-out sensitivity analyses, adjusted within-R^2 for configuration remained higher than that for composition, indicating that the comparison was not driven by any single subbasin.

Grouped cross-validation using Random Forest, XGBoost, and LightGBM provided consistent predictive evidence (Fig. 6b). Mean out-of-fold R^2 values for the composition, configuration, and combined models were 0.374, 0.428, and 0.462 for SRSR and 0.022, 0.186, and 0.197 for SDR, respectively. Configuration models outperformed composition models across all three algorithms, with a particularly large difference for SDR, indicating that configuration contained more information for within-subbasin variation and stronger transferability to subbasins excluded from model training.

SHAP importance further identified the specific metrics underlying this configuration advantage (Fig. 6c, d; Table 3). The four highest-ranked metrics for SRSR were Impervious_COHESION, Forest_LPI, Impervious_LPI, and Impervious_AI, whereas those for SDR were Forest_LPI, Impervious_LPI, Impervious_AI, and Impervious_COHESION; all were class-level configuration metrics. Among composition metrics, Impervious_PLAND remained highly ranked for both responses, and Forest_PLAND was among the top 10 for SRSR. Overall, landscape composition represented the

basic land-cover context of sediment processes, whereas landscape configuration captured additional information on patch dominance, aggregation, and spatial connectivity that was not represented by land-cover proportions alone.

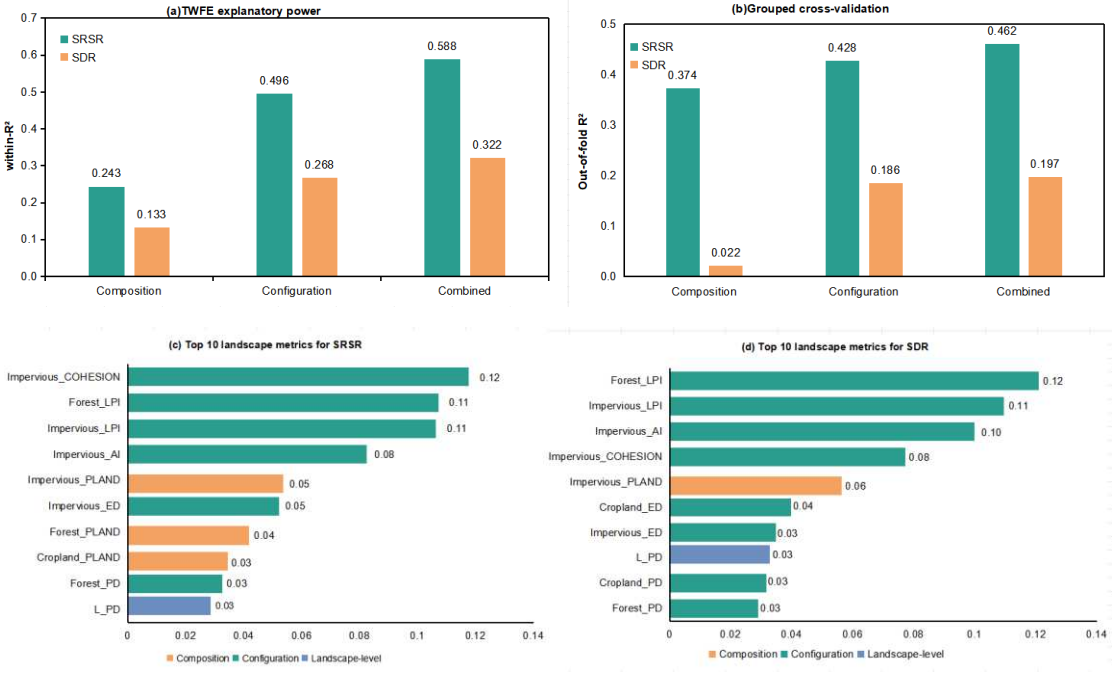


Fig. 6 Complementary evidence for the relative importance of landscape composition and configuration in explaining sediment retention and delivery

(a) Within-R² of two-way fixed-effects models using landscape composition, configuration, and their combination; (b) mean out-of-fold R² from grouped cross-validation across Random Forest, XGBoost, and LightGBM models; (c) mean normalized SHAP importance of the top 10 landscape metrics for SRSR; and (d) corresponding results for SDR. Grouped cross-validation was performed by subbasin. SHAP importance was averaged across the three machine-learning algorithms after within-model normalization

Table 3 Top-ranked landscape metrics for SRSR and SDR identified by ensemble machine-learning models

Response	SHAP rank	Landscape metric	Metric class	Landscape dimension	Mean model rank	Normalized SHAP
SRSR	1	Impervious_COHESION	Class-level configuration	Cohesion/connectivity	3.0	0.1175
	2	Forest_LPI	Class-level configuration	Patch dominance	2.3	0.1072
	3	Impervious_LPI	Class-level configuration	Patch dominance	2.3	0.1062
	4	Impervious_AI	Class-level configuration	Aggregation	4.0	0.0823
	5	Impervious_PLAND	Composition	Composition	6.0	0.0536
	6	Impervious_ED	Class-level configuration	Edge structure	6.3	0.0523
	7	Forest_PLAND	Composition	Composition	9.3	0.0418
	8	Cropland_PLAND	Composition	Composition	9.3	0.0344

	9	Forest_PD	Class-level configuration	Fragmentation	13.3	0.0326
	10	L_PD	Landscape-level configuration	Fragmentation	12.0	0.0285
SDR	1	Forest_LPI	Class-level configuration	Patch dominance	1.7	0.1209
	2	Impervious_LPI	Class-level configuration	Patch dominance	2.7	0.1096
	3	Impervious_AI	Class-level configuration	Aggregation	3.0	0.0998
	4	Impervious_COHESION	Class-level configuration	Cohesion/connectivity	3.7	0.0773
	5	Impervious_PLAND	Composition	Composition	6.3	0.0564
	6	Cropland_ED	Class-level configuration	Edge structure	13.3	0.0398
	7	Impervious_ED	Class-level configuration	Edge structure	9.0	0.0348
	8	L_PD	Landscape-level configuration	Fragmentation	9.0	0.0329
	9	Cropland_PD	Class-level configuration	Fragmentation	12.0	0.0317
	10	Forest_PD	Class-level configuration	Fragmentation	14.0	0.0291

Note: Normalized SHAP importance was averaged across Random Forest, XGBoost, and LightGBM after within-model normalization. Mean model rank is the average variable rank across the three algorithms. Response shape is evaluated separately using TWFE-RCS and is therefore not reported in this table

3.3.2 Responses and nonlinear characteristics of key landscape metrics

Across the 24 TWFE-RCS relationships between the 12 key landscape metrics and SRSR/SDR, 17 showed significant overall associations after FDR correction, and five showed significant nonlinear components (Table 4; Online Resource 2). Thus, most key metrics were statistically associated with sediment retention or delivery, whereas clear nonlinearity was confined to a subset of relationships.

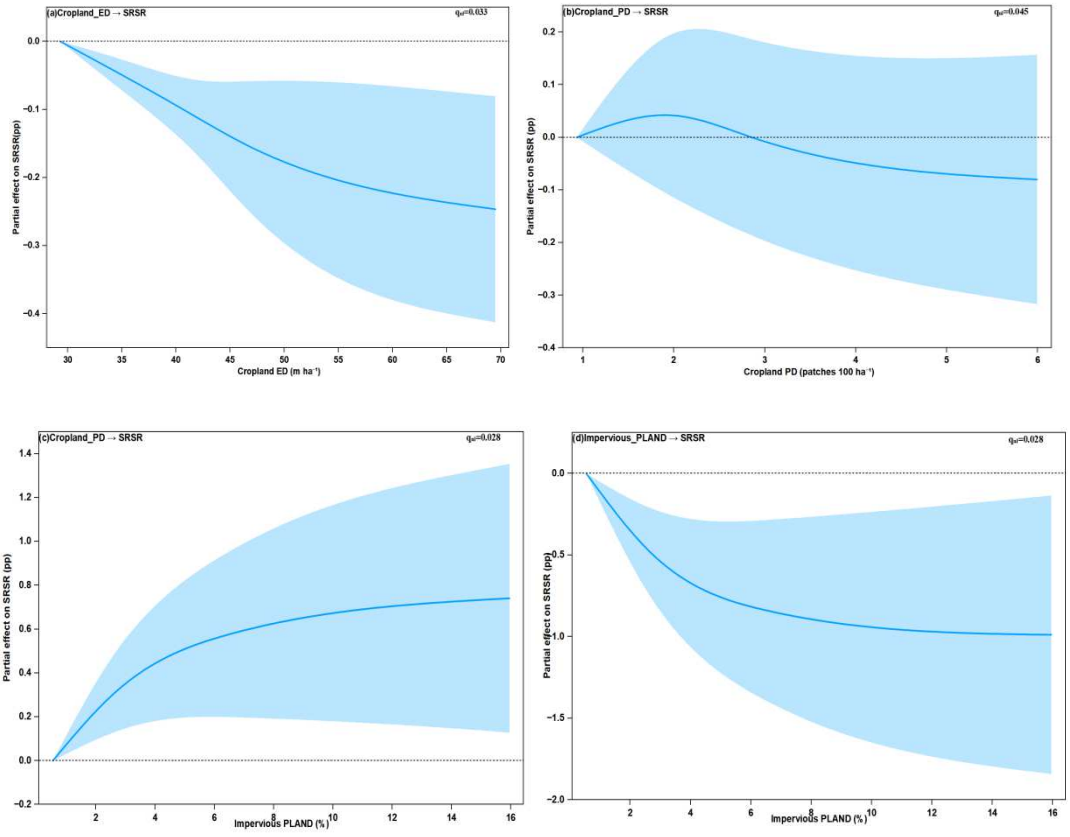
For SRSR, Cropland_ED, Cropland_PD, and Impervious_PLAND exhibited significant nonlinear responses (Fig. 7a–c). Higher Cropland_ED was generally associated with lower SRSR, with the response flattening at higher values. Cropland_PD showed an inverted U-shaped relationship, with a local maximum at approximately 1.91 patches 100 ha^{-1}. Impervious_PLAND showed a nonlinear positive relationship with SRSR, with diminishing increases at higher values. For SDR, both Impervious_PLAND and Impervious_ED showed nonlinear decreases that gradually flattened as the metrics increased (Fig. 7d–e).

Table 4 Response forms of the 12 key landscape metrics to SRSR and SDR identified by TWFE-RCS

Landscape metric	Type	SRSR response	SDR response
Forest_PLAND	Composition	Overall association	Overall association
Cropland_PLAND		n.s.	Overall association
Impervious_PLAND		Nonlinear increase	Nonlinear decrease
Forest_LPI	Configuration	n.s.	Overall association

Landscape metric	Type	SRSR response	SDR response
Forest_PD		n.s.	n.s.
Cropland_ED		Nonlinear decrease	Overall association
Cropland_PD		Inverted U-shaped	n.s.
Impervious_LPI		Overall association	n.s.
Impervious_AI		Overall association	Overall association
Impervious_COHESION		Overall association	n.s.
Impervious_ED		Overall association	Nonlinear decrease
L_PD		Overall association	Overall association

Note:*"Overall association" indicates a significant overall association after BH-FDR correction ($q_{overall}<0.05$) without significant evidence of nonlinearity ($q_{nonlinear}\geq0.05$). "Nonlinear" indicates that both the overall association and nonlinear component were significant after BH-FDR correction. n.s., no significant overall association after FDR correction; Comp., landscape composition; Config., landscape configuration*



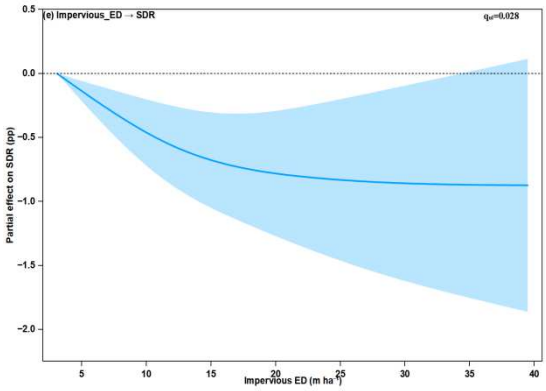


Fig. 7 Nonlinear responses of sediment retention and delivery to key landscape metrics
Curves represent partial effects estimated from two-way fixed-effects restricted cubic spline models relative to the 5th percentile of each metric, and shaded areas indicate 95% confidence intervals. (a) Cropland_ED–SRSR;(b)Cropland_PD–SRSR;(c)Impervious_PLAND–SRSR; (d) Impervious_PLAND–SDR; and (e) Impervious_ED–SDR. q_{nl} denotes the BH-FDR-adjusted significance of the nonlinear spline terms. The local peak shown in (b) represents a response feature within the observed data range rather than a universal ecological threshold

3.4 Spatially varying and context-dependent landscape effects

3.4.1 Subbasin-specific effects of key landscape metrics

Random-slope analyses of the 12 key landscape metrics showed varying degrees of among-subbasin heterogeneity in their relationships with SRSR and SDR. To summarize contrasting forms of spatial heterogeneity, Forest_PLAND, Impervious_LPI, and L_PD were selected as representative metrics of landscape composition, class-level configuration, and landscape-level configuration, respectively.

Forest_PLAND showed the clearest variation in effect direction. Associations corresponding to higher SRSR and lower SDR were concentrated mainly in southwestern and southern subbasins, whereas opposite directions occurred in parts of the northern and central basin, indicating strong spatial heterogeneity in the relationship of Forest_PLAND with sediment retention and delivery. Impervious_LPI also showed pronounced spatial heterogeneity. Positive associations with SRSR occurred mainly in northern, western, and some central subbasins, whereas negative associations occurred in parts of the south and southeast. Associations with SDR were predominantly negative, but their magnitude varied substantially among subbasins without a consistent spatial gradient. In contrast, the direction of L_PD effects was more stable: higher L_PD generally corresponded to lower SRSR and, in most subbasins, higher SDR. Spatial variation was expressed mainly in effect magnitude rather than direction, with stronger effects in northern–central and some western areas and weaker effects in parts of the south.

Overall, the spatial stability of landscape–process relationships differed among metrics. Effect directions for Forest_PLAND and Impervious_LPI varied among subbasins, whereas those for L_PD were comparatively consistent, indicating that the statistical associations of the former metrics were more context dependent, while the relationship between landscape-level fragmentation and sediment processes was more spatially consistent.

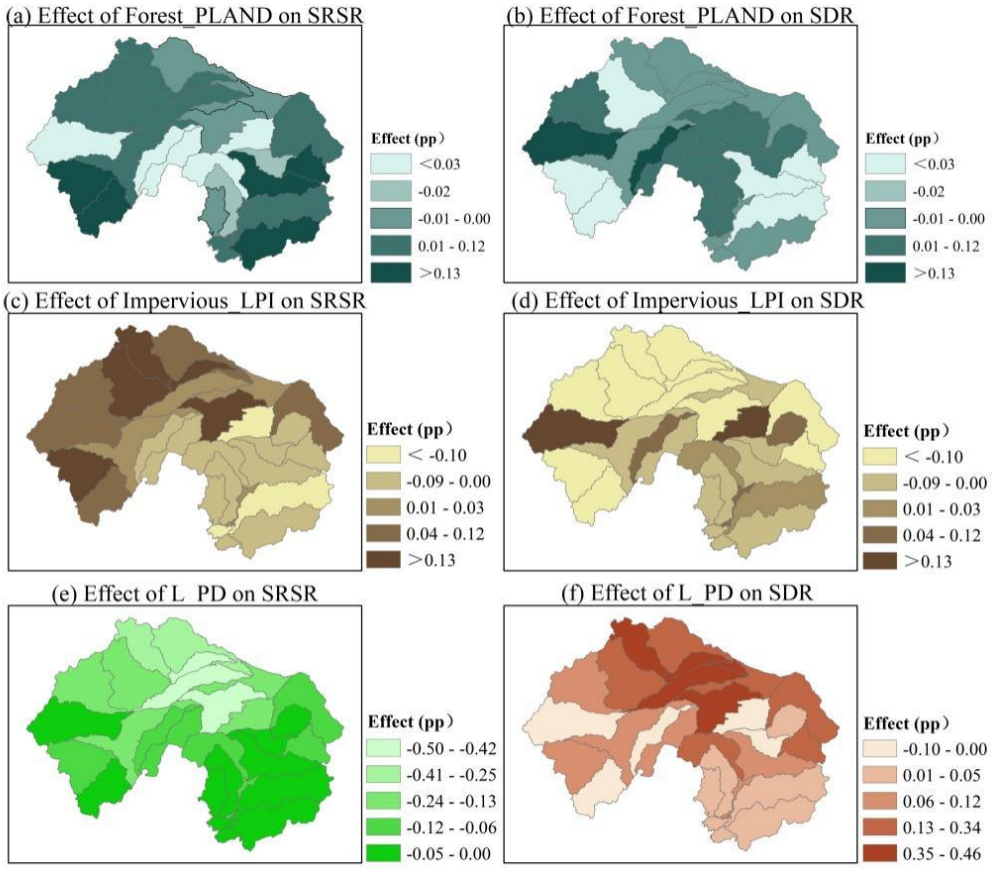


Fig. 8 Subbasin-specific effects of three representative landscape metrics on SRSR and SDR
(a) Forest_PLAND effect on SRSR; (b) Forest_PLAND effect on SDR; (c) Impervious_LPI effect on SRSR; (d) Impervious_LPI effect on SDR; (e) L_PD effect on SRSR; and (f) L_PD effect on SDR. Effect values represent the model-predicted change in SRSR or SDR when each landscape metric increases from the 10th to the 90th percentile of its time series within a given subbasin, expressed in percentage points (pp). Positive and negative values indicate increases and decreases in the response variable, respectively. SRSR and SDR maps for each metric use the same class breaks, whereas class ranges differ among metrics

3.4.2 Landscape-context dependence of subbasin-specific effects

To further characterize spatial variation in key landscape associations, subbasin-specific effects of all key landscape metrics were related to long-term land-use background. Significant landscape-context dependence was supported mainly for SRSR. After FDR correction, four relationships remained significant: the effect of Impervious_LPI on SRSR became weaker as impervious-surface proportion increased; the negative effect of L_PD on SRSR became stronger with increasing grassland proportion; in contrast, higher impervious-surface proportion was associated with a stronger L_PD effect on SRSR; and the positive effect of Forest_PLAND on SRSR was stronger in subbasins with higher forest proportion (Fig. 9). By contrast, evidence for landscape-context dependence was weaker for SDR. Although the Impervious_ED effect varied with Impervious_PLAND and the Forest_PLAND effect varied with Forest_PLAND background, neither relationship remained significant after FDR correction. Overall, statistical support for long-term context dependence of landscape–process relationships was clearer for sediment retention than for sediment delivery.

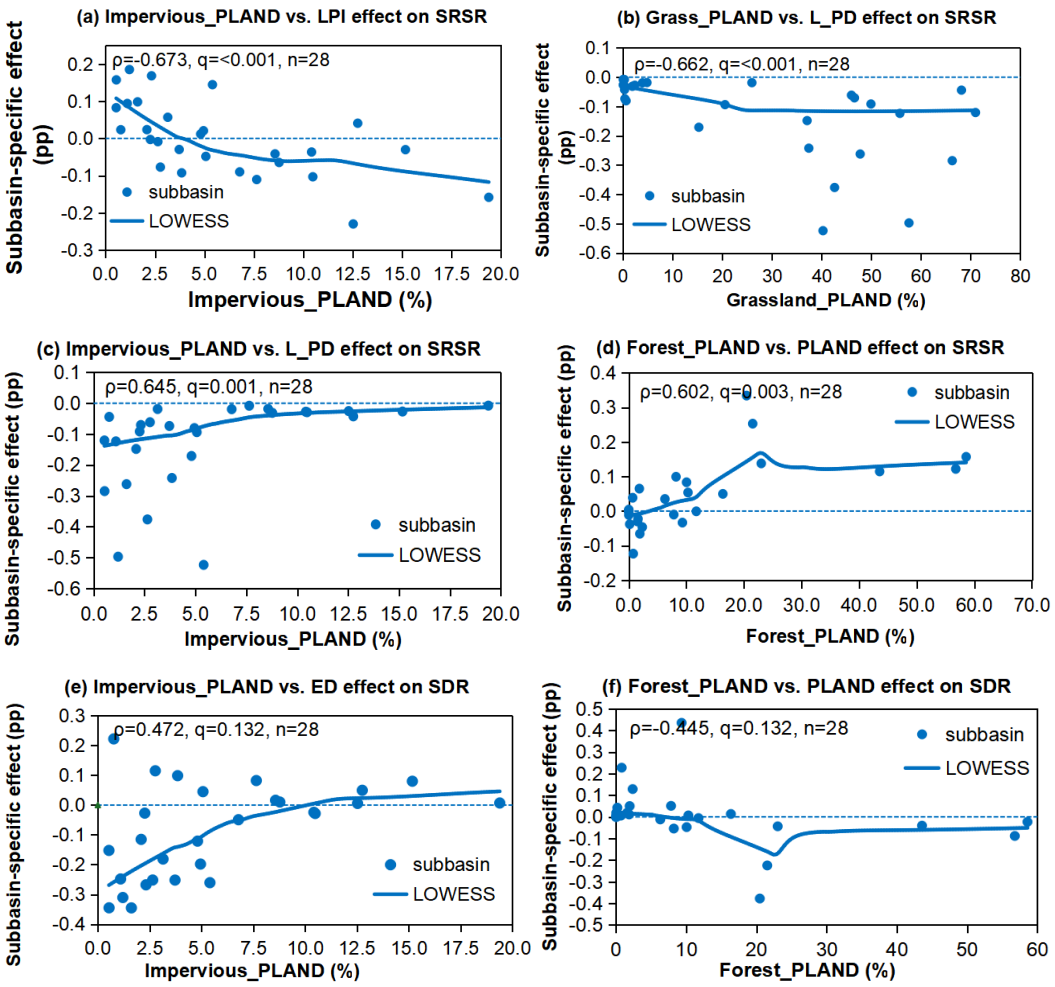


Fig. 9 Relationships between long-term land-use background and subbasin-specific effects of key landscape metrics

(a) Impervious-surface proportion and the effect of Impervious_LPI on SRSR; (b) grassland proportion and the effect of L_PD on SRSR; (c) impervious-surface proportion and the effect of L_PD on SRSR; (d) forest proportion and the effect of Forest_PLAND on SRSR; (e) impervious-surface proportion and the effect of Impervious_ED on SDR; and (f) forest proportion and the effect of Forest_PLAND on SDR. Points represent individual subbasins and lines show LOWESS smooths. denotes Spearman's rank correlation coefficient and the BH-FDR-adjusted significance level

4. Discussion

4.1 Why does landscape configuration provide information beyond composition?

Our results show that both landscape composition and configuration were associated with variation in SRSR and SDR, but configuration retained substantially more independent explanatory information after accounting for composition. Land-cover proportions primarily describe the amount of different potential sediment source and sink types, whereas patch aggregation, fragmentation, edge structure, and spatial position further characterize how these landscape elements are spatially organized. Consequently, land-cover proportions alone may be insufficient to represent sediment processes with strong spatial-transfer characteristics (Bakker et al., 2008; Yang et al., 2012; Zhang et al., 2024). The additional information provided by configuration may reflect its ability to represent source–sink–pathway structure and sediment connectivity. Similar land-cover proportions can correspond to very different patch arrangements, and therefore to different patterns of runoff concentration, sediment interception, and source-to-stream connectivity. In this sense, landscape composition primarily describes how much potential sediment source and sink area is present, whereas landscape

configuration describes how these elements are organized and connected, which may be closely associated with differences in sediment delivery efficiency (Vigiak et al., 2012; Cavalli et al., 2013; Liu et al., 2021).

Responses of the key configuration metrics were consistent with this interpretation. Forest_LPI represents the relative size and dominance of the largest forest patch, Cropland_ED characterizes cropland edges and land-cover interfaces, Impervious_LPI represents dominance of the largest impervious patch, and L_PD describes landscape-level fragmentation. These metrics therefore capture spatial relationships among sediment-source areas, resistance patches, and potential transport pathways rather than land-cover quantity alone. Landscape configuration should thus be viewed as complementary to, rather than a substitute for, landscape composition because it adds information on spatial organization, pathways, and connectivity that is not represented by area proportions alone. This interpretation is consistent with the additional explanatory and predictive information observed for both SRSR and SDR.

4.2 Nonlinearity, spatial heterogeneity, and landscape-context dependence of pattern–process relationships

Landscape–process relationships for sediment retention and delivery were not universally characterized by complex nonlinearity. Most key metrics showed significant and relatively stable overall associations, whereas only a subset remained significantly nonlinear after multiple-testing correction, mainly involving cropland edge and fragmentation characteristics and impervious-surface amount and edge structure. Thus, the importance of landscape pattern does not depend on the presence of a distinct threshold. For several configuration metrics, relationships changed progressively along landscape-structure gradients, whereas clear marginal changes or local turning points occurred only for specific landscape dimensions. This pattern is consistent with the continuous and spatially cumulative nature of sediment transfer, which is related not only to local erosion but also to resistance and connectivity along transport pathways (Vigiak et al., 2012; Cavalli et al., 2013).

At the same time, relationships between individual landscape metrics and sediment processes were not constant among subbasins, indicating that watershed-average relationships may not fully represent local pattern–process responses(Zheng et al., 2026). Information contained in landscape configuration extends beyond individual patches to the spatial connections among sediment-source areas, resistance elements, and stream networks; consequently, statistical associations may vary with surrounding land-use context and pre-existing connectivity. Previous studies have shown that land use and its spatial distribution can alter sediment connectivity and are associated with differences in sediment delivery and yield, while hillslope–channel coupling also varies across topographic and landscape settings (Liu et al., 2021; Cavalli et al., 2013). Recent watershed studies likewise emphasize differentiated relationships between multiple dimensions of landscape heterogeneity and erosion or sediment yield (Zhang et al., 2024). Therefore, similar changes in a landscape metric need not correspond to the same sediment response, and their relationships may depend on landscape context and the transport network.

This spatial heterogeneity is particularly relevant for understanding differences between SRSR and SDR. SRSR more directly represents sediment retention within subbasins, and its dependence on local landscape composition, edge structure, and fragmentation may therefore be more apparent. By contrast, SDR represents the efficiency with which eroded sediment is delivered to stream networks and outlets, and its spatial variation may additionally integrate hillslope–channel connectivity, transport distance, and topographic conditions. Previous studies have shown that even highly connected hillslopes may be followed by low-gradient channel reaches or other depositional units that reduce

further sediment transfer (Cavalli et al., 2013), while relationships between land-use change and sediment yield may be amplified or weakened by changes in connectivity (Liu et al., 2021). Thus, rather than seeking a single landscape threshold, identifying the spatial contexts in which pattern–process relationships strengthen or weaken may provide a more informative view of their context dependence.

4.3 Implications for landscape management and study limitations

These results suggest that watershed landscape management should not focus solely on the proportions of forest, cropland, and impervious surfaces, but should also consider patch dominance, edge structure, aggregation, and landscape-level fragmentation, thereby incorporating both landscape composition and configuration into assessment frameworks. Previous work has similarly emphasized the need to consider composition and configuration jointly in erosion and sediment management (Zhang et al., 2024). In the context of this study, forest management could consider the spatial integrity of dominant patches in addition to overall cover, while cropland and impervious-surface management could account for edge expansion, aggregation, and spatial relationships with potential sediment-transport pathways.

Spatial heterogeneity and landscape-context dependence of pattern–process relationships further indicate that identical landscape-optimization criteria may not be appropriate for all subbasins. A more differentiated approach would consider dominant land-use context and key configuration characteristics within each subbasin, with particular attention to locations that may modify source–sink–pathway relationships and sediment connectivity. Previous studies have reported that land-use pattern change and ecological restoration can influence sediment export through changes in sediment connectivity (Liu et al., 2021), and that subbasins may exhibit contrasting water–sediment responses depending on the magnitude of landscape change (Qin et al., 2025).

Several limitations should be acknowledged. InVEST-SDR provides a spatially explicit framework for assessing sediment retention and delivery at the watershed scale, but its process representation remains a relatively simplified empirical approximation and therefore carries uncertainty in representing complex sediment sources and transport processes (Hamel et al., 2015). In addition, the nonlinear responses, random-slope variation, and landscape-context relationships identified here represent conditional statistical associations and should not be interpreted directly as causal mechanisms. Future studies could combine field-observed sediment data, more direct measures of hillslope–stream connectivity, and multiscale landscape analyses to further evaluate potential response transitions, spatial heterogeneity, and their underlying process basis.

5. Conclusions

This study examined relationships between landscape pattern and sediment retention and delivery from the complementary perspectives of landscape composition and configuration. Both dimensions provided explanatory information, but landscape configuration retained greater independent explanatory and predictive contributions after accounting for composition. Configuration metrics such as Forest_LPI, Impervious_LPI, Cropland_ED, and L_PD further represented spatial characteristics related to patch dominance, edge structure, aggregation, and landscape-level fragmentation, indicating that land-cover proportions alone are insufficient to fully characterize landscape pattern–sediment process relationships at the watershed scale.

Relationships between key landscape metrics and sediment processes showed pronounced spatial heterogeneity, whereas clear nonlinear responses were confined to a subset of relationships. Some subbasin-specific effects were significantly associated with long-term landscape context, with stronger

statistical support for landscape-context dependence in SRSR than in SDR.

Overall, understanding sediment retention and delivery requires consideration of landscape composition, configuration, and landscape context together. Watershed assessment and management should therefore move beyond land-cover proportions alone and account for differences in spatial configuration and landscape context among subbasins.

Reference

Bakker MM, Govers G, van Doorn A, Quétier F, Chouvardas D, Rounsevell M (2008) The response of soil erosion and sediment export to land-use change in four areas of Europe: The importance of landscape pattern. Geomorphology 98:213–226. https://doi.org/10.1016/j.geomorph.2006.12.027.

Borselli L, Cassi P,Torri D (2008) Prolegomena to sediment and flow connectivity in the lands cape: A GIS and field numerical assessment. CATENA 75:268–277.https://doi.org/10.1016/j. catena.2008.07.006.

Bracken LJ, Turnbull L, Wainwright J, Bogaart P (2015) Sediment connectivity: A framework for understanding sediment transfer at multiple scales. Earth Surface Processes and Landforms 40:177–188. https://doi.org/10.1002/esp.3635.

Cavalli M, Trevisani S, Comiti F, Marchi L (2013) Geomorphometric assessment of spatial sed iment connectivity in small Alpine catchments. Geomorphology 188:31–41.https://doi.org/10. 1016/j.geomorph.2012.05.007.

Desquilbet L, Mariotti F (2010) Dose-response analyses using restricted cubic spline functions i n public health research. Statistics in Medicine 29:1037–1057. https://doi.org/10.1002/sim.38 41

Durrleman S, Simon R (1989) Flexible regression models with cubic splines. Statistics in Medicine 8:551–561. https://doi.org/10.1002/sim.4780080504

Fryirs K (2013) (Dis)Connectivity in catchment sediment cascades: A fresh look at the sedimen t delivery problem. Earth Surface Processes and Landforms 38:30–46. https://doi.org/10.100 2/esp.3242.

Hamel P, Chaplin-Kramer R, Sim S, Carina Mueller (2015) A new approach to modeling the s ediment retention service (InVEST 3.0): Case study of the Cape Fear catchment, North Ca rolina, USA.Science of the Total Environment,524-525,166-177.https://doi.org/10.1016/j.scitot env.2015.04.027.

Levin SA (1992) The problem of pattern and scale in ecology: The Robert H. MacArthur Awa rd Lecture. Ecology 73:1943–1967. DOI: 10.2307/1941447

Liu W, Shi C, Ma Y, Li H, Ma X (2021) Land use and land cover change-induced changes o f sediment connectivity and their effects on sediment yield in a catchment on the Loess P lateau in China. CATENA 207:105688. https://doi.org/10.1016/J.CATENA.

Mcgarigal K, Marks B J (1995) FRAGSTATS—Spatial Pattern Analysis Program for Quantifyin g Landscape Structure.USDA Forest Service - General Technical Report PNW, 351.DOI:10. 2737/PNW-GTR-351.

Pickett STA, Cadenasso ML (1995) Landscape ecology: Spatial heterogeneity in ecological syst ems. Science 269:331–334. DOI: 10.1126/science.269.5222.331

Qin Y, Shi P, Hu Y, Li Q, Wang Y, Wang Q, Zhou D (2024) Landscape indices explain differ ent responses of runoff and sediment yield to land use/cover change on the Loess Plateau, China.Catena,2025,249108674-108674.https://doi.org/10.1016/J.CATENA.2024.108674.

Shi ZH, Ai L, Li X,Huang XD, Wu GL, Liao W (2013) Partial least-squares regression for lin king land-cover patterns to soil erosion and sediment yield in watersheds. Journal of Hydr ology 498:165–176.https://doi.org/10.1016/j.jhydrol.2013.06.031.

Turner MG (1989) Landscape ecology: The effect of pattern on process. Annual Review of Ec ology and Systematics 20:171–197. DOI: 10.1146/annurev.es.20.110189.001131

Uuemaa E, Antrop M, Roosaare J, Marja R, Mander Ü (2009). Landscape metrics and indices: An overview of their use in landscape research. Living Reviews in Landscape Research, 3, 1.https://doi.org/10.12942/LRLR-2009-1.

Vigiak O, Borselli L, Newham L T H, McInnes J, Roberts A M (2012).Comparison of concept ual landscape metrics to define hillslope-scale sediment delivery ratio. Geomorphology, 138 (1), 74–88.https://doi.org/10.1016/j.geomorph.2011.08.026.

Valladares-Castellanos M, de Jesús Crespo R, Douthat T (2026) The role of landscape composi tion and configuration on watershed nutrient exports: A 60-year multiscale study in Puerto Rico. Landscape Ecology 41:58.https://doi.org/10.1007/S10980-026-02318-X.

Walling DE (1983) The sediment delivery problem. Journal of Hydrology 65:209–237. DOI: 10. 1016/0022-1694(83)90217-2

Weller DE, Baker ME, King RS (2023) New methods for quantifying the effects of catchment spatial patterns on aquatic responses. Landscape Ecology 38:2687–2703. https://doi.org/10. 1007/S10980-023-01706-X.

Yang M, Li X, Hu Y, He X (2012) Assessing effects of landscape pattern on sediment yield using sediment delivery distributed model and a landscape indicator. Ecological Indicators 22:38–52. https://doi.org/10.1016/j.ecolind.2011.08.023.

Zhang H, Lv J, Bao Y, Tang Q, Collins AL,Khurram D, He X (2024) Linking soil erosion and sediment yield with landscape heterogeneity: Exploration using the lower Jinsha River Basin, China. Journal of Hydrology 631:130729.https://doi.org/10.1016/J.JHYDROL.2024.130729.

Zheng D, Liu H, Yan C, Rong Z, Nian T (2026) Risk assessment for regional submarine landslides integrating AutoML with AHP-EWM approach: a case study from the South-West Iberian sea. Georisk: Assessment and Management of Risk for Engineered Systems and Geohazards 20:672–695. https://doi.org/10.1080/17499518.2026.2619867

Statements and Declarations

Funding

This work was supported by National Natural Science Foundation of China,Liaoning Provincial Department of Education Project (Grant numbers No. 41701208 and LJ212510165028).

Competing Interests

The authors have no relevant financial or non-financial interests to disclose.

Author Contributions

All authors contributed to the study conception and design. Material preparation, data collection and analysis were performed by Leting Lyu,Yan Niu,MengjiaoHou,Defeng Zheng,Feipeng Ren. The first draft of the manuscript was written by Leting Lyu,Yan Niu and all authors commented on previous versions of the manuscript. All authors read and approved the final manuscript.

Data Availability

All data supporting this study are included in the article and its supplementary materials.

699 Online Resource 1. Associations between long-term land-use background and subbasin-specific effects
700 of key landscape metrics

Response	Subbasin-specific effect	Land-use background	Spearman ρ	p	FDR q
SRSR	Impervious_LPI	Impervious_PLAND	**−0.656**	<0.001	**0.0023**
	Forest_PLAND	Forest_PLAND	**0.606**	<0.001	**0.0047**
	L_PD	Impervious_PLAND	**0.513**	0.0052	**0.0213**
	L_PD	Grassland_PLAND	**−0.509**	0.0057	**0.0213**
	Impervious_AI	Impervious_PLAND	0.440	0.0191	0.0573
	Impervious_COHESION	Impervious_PLAND	−0.419	0.0266	0.0624
	Impervious_ED	Impervious_PLAND	−0.407	0.0317	0.0624
	Impervious_PLAND	Impervious_PLAND	−0.403	0.0333	0.0624
	L_PD	Forest_PLAND	0.323	0.0931	0.1552
	Cropland_ED	Cropland_PLAND	0.280	0.1495	0.2242
	L_PD	Cropland_PLAND	0.270	0.1649	0.2249
	Cropland_PLAND	Cropland_PLAND	−0.159	0.4182	0.5227
	Forest_LPI	Forest_PLAND	−0.121	0.5406	0.6238
	Forest_PD	Forest_PLAND	0.066	0.7377	0.7503
	Cropland_PD	Cropland_PLAND	0.063	0.7503	0.7503
SDR	Impervious_ED	Impervious_PLAND	0.513	0.0053	0.0709
	Forest_PLAND	Forest_PLAND	−0.482	0.0095	0.0709
	Impervious_PLAND	Impervious_PLAND	0.407	0.0317	0.1587
	Impervious_COHESION	Impervious_PLAND	0.347	0.0704	0.2641
	Impervious_LPI	Impervious_PLAND	0.317	0.0997	0.2992
	Cropland_PLAND	Cropland_PLAND	−0.282	0.1462	0.3654
	L_PD	Forest_PLAND	−0.223	0.2533	0.5211
	L_PD	Impervious_PLAND	−0.212	0.2779	0.5211
	Cropland_ED	Cropland_PLAND	−0.190	0.3316	0.5329
	L_PD	Grassland_PLAND	0.166	0.3974	0.5329
	Impervious_AI	Impervious_PLAND	0.164	0.4037	0.5329
	Cropland_PD	Cropland_PLAND	−0.157	0.4263	0.5329
	L_PD	Cropland_PLAND	−0.108	0.5830	0.6727
	Forest_LPI	Forest_PLAND	−0.094	0.6347	0.6800
	Forest_PD	Forest_PLAND	−0.050	0.7991	0.7991

701
702

Online Resource 2. Complete TWFE-RCS results for the 24 relationships between key landscape metrics and sediment responses

Metric	Type	Response	Overall F	Overall p	Overall q	Nonlinear F	Nonlinear p	Nonlinear q	Q5–Q95 Δ, pp (95% CI)
Forest_PLAND	Comp.	SRSR	36.638	<0.0001	**<0.0001**	4.952	0.0147	0.0589	+1.928 (1.443, 2.413)
		SDR	15.062	<0.0001	**<0.0001**	3.413	0.0477	0.1144	−1.642 (−2.371, −0.913)
Cropland_PLAND	Comp.	SRSR	0.891	0.4583	0.5000	0.645	0.5327	0.6088	−0.217 (−0.626, 0.192)
		SDR	4.325	0.0130	**0.0207**	0.520	0.6002	0.6548	+0.725 (0.183, 1.268)
Impervious_PLAND	Comp.	SRSR	5.010	0.0069	**0.0150**	7.409	0.0027	**0.0284**	+0.741 (0.128, 1.354)
		SDR	7.276	0.0010	**0.0048**	8.549	0.0013	**0.0284**	−0.988 (−1.841, −0.135)
Forest_LPI	Config.	SRSR	0.228	0.8761	0.8761	0.339	0.7153	0.7464	−0.112 (−0.581, 0.358)
		SDR	3.635	0.0253	**0.0357**	1.572	0.2261	0.3192	−0.461 (−1.319, 0.398)
Forest_PD	Config.	SRSR	0.417	0.7423	0.7745	0.027	0.9730	0.9730	−0.101 (−0.288, 0.086)
		SDR	1.195	0.3305	0.3777	0.680	0.5153	0.6088	+0.316 (−0.079, 0.710)
Cropland_ED	Config.	SRSR	7.005	0.0012	**0.0050**	6.366	0.0054	**0.0326**	−0.246 (−0.412, −0.080)
		SDR	3.761	0.0224	**0.0335**	2.462	0.1042	0.1924	+0.309 (0.097, 0.522)
Cropland_PD	Config.	SRSR	5.270	0.0054	**0.0130**	5.581	0.0094	**0.0450**	−0.080 (−0.317, 0.157)
		SDR	2.818	0.0579	0.0772	1.911	0.1674	0.2511	+0.160 (−0.099, 0.420)
Impervious_LPI	Config.	SRSR	4.828	0.0081	**0.0150**	3.254	0.0542	0.1182	+0.114 (−0.347, 0.574)
		SDR	2.667	0.0678	0.0856	3.952	0.0312	0.0937	−0.495 (−0.898, −0.092)
Impervious_AI	Config.	SRSR	9.095	0.0003	**0.0015**	4.026	0.0295	0.0937	+0.216 (−0.215, 0.646)
		SDR	4.850	0.0079	**0.0150**	3.757	0.0363	0.0969	−1.039 (−2.041, −0.038)

Metric	Type	Response	Overall F	Overall p	Overall q	Nonlinear F	Nonlinear p	Nonlinear q	Q5–Q95 Δ, pp (95% CI)
Impervious_COHESION	Config.	SRSR	4.650	0.0096	**0.0164**	2.171	0.1336	0.2137	+0.255 (−0.010, 0.520)
		SDR	2.407	0.0892	0.1070	2.293	0.1203	0.2061	−0.463 (−0.820, −0.107)
Impervious_ED	Config.	SRSR	19.744	<0.0001	**<0.0001**	1.427	0.2576	0.3329	+1.421 (0.962, 1.881)
		SDR	5.642	0.0039	**0.0104**	7.002	0.0035	**0.0284**	−0.873 (−1.862, 0.116)
L_PD	Config.	SRSR	6.468	0.0019	**0.0058**	1.402	0.2635	0.3329	−0.415 (−0.613, −0.217)
		SDR	6.567	0.0018	**0.0058**	3.036	0.0647	0.1294	+0.532 (0.199, 0.866)

704

Supplementary Files

This is a list of supplementary files associated with this preprint. Click to download.

- ESM1..pdf
- ESM2..pdf